

Review

# A Switching Hybrid Dynamical System: Toward Understanding Complex Interpersonal Behavior

Yuji Yamamoto <sup>1,†,\*</sup>, Akifumi Kijima <sup>2,‡</sup>, Motoki Okumura <sup>3,‡</sup>, Keiko Yokoyama <sup>1,†,‡</sup> and Kazutoshi Gohara <sup>4,‡</sup>

<sup>1</sup> Research Center of Health, Physical Fitness, and Sports, Nagoya University, Nagoya, Japan 1; yamamoto@htc.nagoya-u.ac.jp

<sup>2</sup> Graduate School of Education, University of Yamanashi, Kofu, Japan 2; akijima@yamanashi.ac.jp

<sup>3</sup> Graduate School of Education, Tokyo Gakugei University, Tokyo, Japan 3; okumura@u-gakugei.ac.jp

<sup>4</sup> Nano Biotechnology, Research Faculty of Engineering, Hokkaido University, Sapporo, Japan 4; gohara@eng.hokudai.ac.jp

\* Correspondence: yamamoto@htc.nagoya-u.ac.jp; Tel.: +81-52-789-3964

† e-mail: yokoyama@htc.nagoya-u.ac.jp

‡ These authors contributed equally to this work.

**Abstract:** Complex human behavior, including interlimb and interpersonal coordination, has been studied from a dynamical system perspective. We review the applications of a dynamical system approach to a sporting activity, which includes continuous, discrete, and switching dynamics. Continuous dynamics identified switching between in- and anti-phase synchronization, controlled by an interpersonal distance of 0.1 m during expert kendo matches, using a relative phase analysis. As discrete dynamics, return map analysis was applied to the time series of movements during kendo matches, and six coordination patterns were classified. Furthermore, state transition probabilities were calculated based on the two states, which clarified the coordination patterns and switching behavior. We introduced switching dynamics with temporal inputs to clarify the simple rules underlying the complex behavior corresponding to switching inputs in a striking action as a non-autonomous system. As a result, we determined that the time evolution of the striking action was characterized as fractal-like movement patterns generated by a simple Cantor set rule with rotation. Finally, we propose a switching hybrid dynamics to understand both court-net sports, as strongly coupled interpersonal competition, and weakly coupled sports, such as martial arts.

**Keywords:** interpersonal coordination, competition, dynamical systems, discrete dynamics, continuous dynamics, sporting activity

## 1. Introduction

Exploring complex human behavior from the perspective of a dynamical system began with an historic experiment by [1]. Three decades later, a new approach has been developed using dynamical system theory and utilities to analyze and simulate complex phenomena, such as human movement, with super-computers. In this article, we review the applications of a dynamical system approach to human behavior, with particular regard to sports activities that require quick decision-making and appropriate execution. We provide applications for continuous dynamics, discrete dynamics, switching dynamics, and switching hybrid dynamics, with a short theoretical review.

Human behavior, particularly the behavior of rhythmic cyclical movements, can be understood as continuous dynamics that can be described using differential equations. In 1665, the Dutch physicist Cristiaan Huygens synchronized two pendulum clocks using the interactions of tiny

vibrations in their common support [2,3]. Synchronizing the two clocks was regarded as entrainment and/or synchronization of the two nonlinear coupled oscillators model. [4] developed the theoretical Haken-Kelso-Bunz (HKB) model to describe the phase transition during the coordinating pattern observed between hands based on synergistics [5] and nonlinear oscillator theory. This model has been applied to intrapersonal and interpersonal coordination [6,7].

Furthermore, group synchrony or coordination has been examined using the Kuramoto model and/or the Kuramoto order parameter [8], concerning synchronized clapping [9] and phase synchronization among rocking chairs in a small group [10,11]. Anti-phase synchronization of the three frogs was analyzed as a phase oscillator model [12]. As another approach, the symmetric Hopf bifurcation theory based on group theory [13] has been applied to investigate the synchronized pattern of three people during a sports activity [14]. These approaches could be regarded as oscillator dynamics; that is, continuous dynamics.

On the other hand, discrete dynamics and/or mapping can be depicted as iterated maps; that is, difference equations describing the time evolution, such as population dynamics with generations or coin flips. The logistic map is a well-known map of how complex, chaotic behavior can arise from very simple quadratic difference equations. A Markov chain in discrete time, which is characterized as a state transition based on the probability distribution of the next state, depends only on the current state as a kind of discrete dynamics, and has been applied to batting a baseball [15] and to squash [16,17]. However, these studies examined predictions in competitive sports performance and did not explore the underlying dynamics. We introduce examples to explore the simple rules underlying a complex human behavior using a Lorenz map; that is, a first return map and a Poincaré map from continuous dynamics to discrete dynamics.

Previous studies have been based on two nonlinear-coupled oscillators; thus, these systems are closed systems with no abrupt changes in external input. We introduce a research result in which switching dynamics with temporal input was applied to continuous striking movements. This model also uses the idea of the Poincaré map. Finally, to explore complex human movement as a dynamical system, we introduce switching hybrid dynamical systems, which include discrete and continuous dynamics with a feedback loop.

## 2. Continuous dynamics

### 2.1. The HKB model

[1] showed that human behavior, particular rhythmic cyclical movement, is a phenomena of entrainment and/or synchronization of two-coupled nonlinear oscillators. In a famous experiment, participants were asked to oscillate their index fingers at a common frequency. The relative phase, which is the difference between the oscillation phases of two fingers, depicts the spatiotemporal pattern of coordination as an order parameter. The coordination mode shows only two steady states, such as  $0^\circ$  relative phase (in-phase mode) and  $180^\circ$  relative phase (anti-phase mode). As movement frequency increases, the anti-phase spontaneously switched to the in-phase mode; however, in-phase did not switch to the anti-phase mode. Below a critical frequency, the system showed bistable behavior with both in- and anti-phase modes; however, above a critical frequency the system showed monostable behavior with only the in-phase mode. The HKB model was developed based on synergistics [5] to explain the phase transition, including hysteresis, critical slowing down, and critical fluctuations using order and control parameters [4,18]. The equation revealed the potential function underlying the spontaneous transition from bistable to monostable behavior. Furthermore, the HKB model for intrapersonal coordination was extended to interpersonal coordination [6,7].

In the interpersonal coordination experiment, cross-spectral coherence and the distribution of the relative phase region were calculated as coordination indices [19–22]. Cross-spectral coherence provides a method to correlate two time series over a range of possible component frequencies. In other words, this analysis reveals the dominant frequencies and/or the strength of the coordination.

76 On the other hand, evaluating the relative phase distribution indicates which relative phase locations  
77 are attractive by identifying the dominant kind of coordination. In this analysis, the distribution  
78 of relative phase angles across nine relative phase regions between  $0^\circ$  and  $180^\circ$  was determined by  
79 calculating the frequency of occurrence of the relative phase angles in each of these regions.

80 Both coordination indices postulate periodic movement, such as that of a hand-held pendulum  
81 [21,22]. However, the behavior of competitive sports players does not always show such periodic  
82 movement. A cross-spectral analysis could not be applied to this kind of time series because of the  
83 abrupt changes and aperiodic behavior. In addition, the relative phase was usually calculated by  
84 point estimates [23] or continuous estimates [24]; however, an aperiodic or arbitrary time series cannot  
85 be calculated using these estimates. To solve this problem, the Hilbert transform [25,26] was applied  
86 to the arbitrary coordination signal in competitive sports to calculate the instantaneous phase.

87 Then, a relative phase analysis using the Hilbert transform was applied to court-net sports,  
88 such as tennis [27–29] and squash [30]. They reported that players' movements frequently switched  
89 between in- and anti-phase synchronization in the direction of the short axis of the court as they took  
90 turns hitting the ball. In addition, [31] proposed the speed scalar product as a collective variable  
91 to describe different patterns during badminton. In these court-net sports, the ball is considered  
92 a physical link to constrain the opponent's movement. These systems of two and/or more players  
93 can be regarded as strongly coupled oscillators [32]. However, it remains unclear whether each player  
94 and/or oscillator could be considered a self-excited oscillation or forced oscillation in court-net sports.

## 95 2.2. The relative phase region reveals the synchronization modes during interpersonal competition

96 As mentioned above, ball movement during court-net sports constrains player movement.  
97 However, in martial arts, such as boxing or fencing, the two players are not joined together physically  
98 and can move freely around, although the players must co-adapt to the opponent's movement.  
99 Consequently, the movements of players can be regarded as self-excited oscillations, and a system  
100 of two players can be considered weakly coupled nonlinear oscillators [8,26,33]. We applied the  
101 distribution from a relative phase analysis to Japanese fencing, which is called kendo, to examine  
102 the synchronization mode during matches [34].

103 We observed 12 kendo matches among six expert members of a university kendo team; all  
104 matches followed official kendo rules. The candidate order parameter was the relative phase angle  
105 of the step toward-away velocity, and the candidate control parameter was the interpersonal distance  
106 between the two players. The interpersonal distance, called "ma'ai", is crucial in kendo, because a  
107 player must simultaneously strike an opponent and avoid the opponent's counterstrike. Scoring a  
108 point (*ippon*) requires an accurate strike on an opponent. Consequently, the players must repeat step  
109 toward-away movements to adjust "ma'ai", and a striking movement, which requires less than 0.4  
110 seconds.

111 The results showed that anti-phase synchronization was clearly dominant at an interpersonal  
112 distance  $< 2.7$  m (near distance). If player A moved toward player B, player B moved away from  
113 player A. However, in-phase synchronization was dominant when interpersonal distance was  $> 3.0$   
114 m (far distance). We focused on the 2.7–3.0 m distance to analyze the phase transition. The frequency  
115 of the relative phase in the 0.1 m range is shown in Figure 1. The results clearly show that higher  
116 anti-phase synchronization occurred at 2.7–2.8 m than at other distances, and this switched to in-phase  
117 synchronization at 2.9–3.0 m, setting a boundary at 2.8–2.9 m. This finding indicates that the players  
118 perceived and understood the need for minute changes on a 0.1 m scale and, consequently, regularly  
119 switched their movement to the appropriate direction or synchronization mode.

120 The distribution of the relative phase analysis revealed switching between the synchronization  
121 modes of interpersonal competition corresponding to the interpersonal distance as the control  
122 parameter. In addition, the synchronization modes changed by learning the interpersonal  
123 competition task using this analysis [35]. However, in this analysis, the distribution of the relative  
124 phases across nine  $20^\circ$  relative phase regions from  $0^\circ$  to  $180^\circ$  was determined, and the resulting

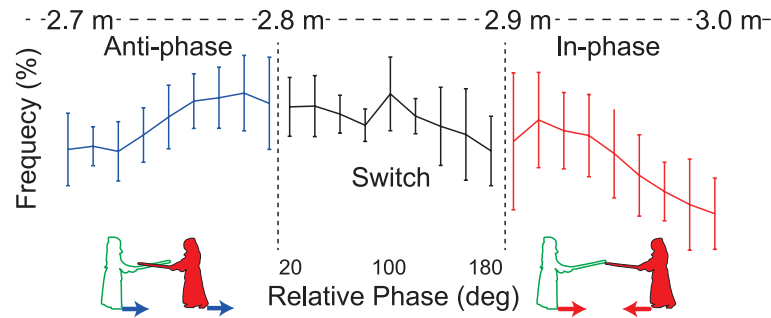


**Figure 1.** Abrupt changes in the interpersonal coordination pattern corresponding to an interpersonal distance of 2.7–3.0 m during kendo. The frequencies of the relative phase per 0.1 m interval at interpersonal distances of 2.7–3.0 m were calculated, and the means and standard deviations are presented. The relative phases were divided into nine ranges ( $20^\circ$ :  $0 - 20^\circ$ ,  $100^\circ$ :  $80 - 100^\circ$ ,  $180^\circ$ :  $160 - 180^\circ$ ). Anti-phase coordination was dominant at interpersonal distances of 2.7–2.8 m; however, in-phase was dominant at interpersonal distances of 2.9–3.0 m. Modified from [34].

125 frequencies of occurrence were calculated. Because of methodological limitations, this approach  
 126 cannot reveal the time evolution in time series data. In other words, the coordination modes can be  
 127 described, but the coordination patterns in a shorter time window cannot be described. Interpersonal  
 128 competition is characterized by aperiodic movements.

### 129 3. Continuous to discrete dynamics: Return map

#### 130 3.1. Lorenz map

131 To describe the time evolution for interpersonal coordination, we introduce a method to explore  
 132 regularity by reducing the dimensionality of continuous dynamics (e.g., three-dimensional flow) to  
 133 discrete dynamics (e.g., two- or one-dimensional). The most popular method is the Lorenz map,  
 134 which was a seminal work that contributed to the foundation of chaos theory [36].

135 The meteorologist, Edward Lorenz, developed a simplified mathematical model for atmospheric  
 136 convection [36]. The model is a system of three ordinary differential equations now known as the  
 137 Lorenz equations:

$$\frac{dx}{dt} = \sigma(y - x) \quad (1)$$

$$\frac{dy}{dt} = x(r - z) - y \quad (2)$$

$$\frac{dz}{dt} = xy - bz \quad (3)$$

138 Here  $x$ ,  $y$ , and  $z$  are proportional to the intensity of convection motion, proportional to the  
 139 temperature difference between the ascending and descending currents, and proportional to  
 140 distortion of the vertical temperature profile from linearity, respectively.  $\sigma$ ,  $r$ , and  $b$  are the system  
 141 parameters. Lorenz focused on “single feature [36, p. 138]”; that is,  $z_n$ , of his three-dimensional  
 142 strange attractor (Figure 2a). Figure 2b shows a time series of  $z(t)$ , and the  $z(t)$  peaks were plotted as  
 143  $z_n$  vs.  $z_{n+1}$  (Figure 2c). The function  $z_{n+1} = f(z_n)$  is called the Lorenz map. The Lorenz map shows  
 144 the road to chaos through the bifurcation [33].

#### 145 3.2. Return map reveals the coordination patterns during interpersonal competition

146 The first return (Lorenz) map was applied to the offensive and defensive maneuvers that occur  
 147 during kendo matches as interpersonal competition [37]. Figure 3a shows the time series of state

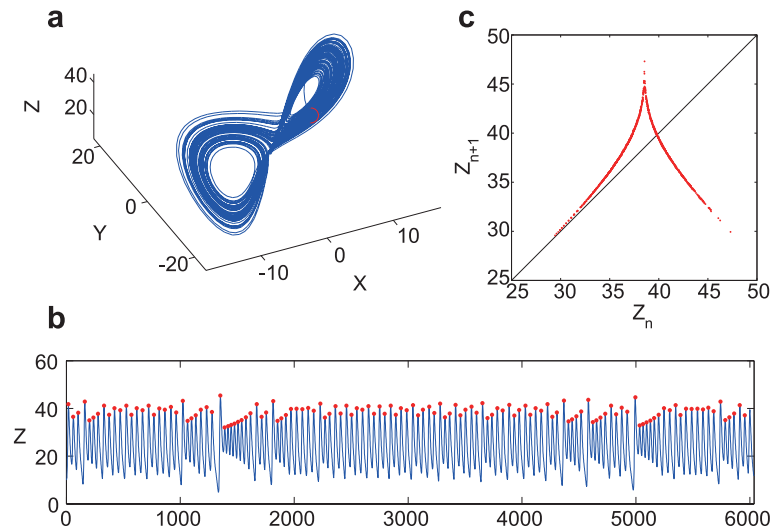


**Figure 2.** Lorenz attractor and Lorenz map. Each parameter is  $\sigma = 10, b = 8/3, r = 28, x_0 = y_0 = z_0 = 10$ . (a) Lorenz attractor in three-dimensional space. (b) Time series of  $z(t)$  and the peaks of  $z(t)$  are shown as red dots. (c) Lorenz map plotted as  $z_n$  vs.  $z_{n+1}$ .

148 variables constituted by interpersonal distance and its velocity. We detected the peaks of the time  
 149 series for interpersonal distance, and the peaks of the state variables were plotted as a return map as  
 150 the present peak  $X_n$  vs. the next peak  $X_{n+1}$  (Figure 3b).

151 The periodicities on such a plot are the intersections with the identity line  $X_n = X_{n+1}$ . These  
 152 intersections are known as attractive fixed points and repellers or saddle points. These attractive  
 153 fixed points are deterministically approached from a direction called the stable direction or manifold,  
 154 and the repellers diverge from these attractive fixed points along the unstable direction or manifold as  
 155 a linear function. Theoretically, we postulated the linear function,  $X_{n+1} = aX_n + b$ . The intersections  
 156 can be classified into two properties depending on the absolute value of  $a$ . When the absolute value of  
 157  $a$  is  $< 1$ ,  $|a| < 1$ , then the intersection is considered to be an attractive fixed point (i.e., an “attractor”).  
 158 When the absolute value of  $a$  is  $> 1$ ,  $|a| > 1$ , then the intersection is referred to as a repellent fixed  
 159 point (i.e., a “repeller”). An attractor can be further classified into two types. When  $0 < a < 1$ , the  
 160 trajectories are asymptotically close to the attractor (Figure 4a). When  $-1 < a < 0$ , the trajectories are  
 161 rotationally close to the attractor (Figure 4b). A repeller also has two types of trajectories:  $1 < a$ , and  
 162  $a < -1$ , corresponding to asymptotical and rotational trajectories, respectively, as shown in Figures  
 163 4c and 4d. Trajectories approach and diverge from points that do not cross the line  $X_n = X_{n+1}$ .  
 164 We postulate that this exponential function,  $X_{n+1} = b \exp(aX_n)$ , and this logarithmic function,  
 165  $X_{n+1} = a \log X_n + b$  (Figure 4e), represent intermittency.

166 As shown in Figure 4, all six predicted types of functions were confirmed in the kendo matches,  
 167 suggesting that the complex offensive and defensive maneuvers were generated by simple rules.  
 168 Furthermore, we detected several functions or patterns during one offensive and defensive scene  
 169 (Figure 4f), indicating that interpersonal coordination switched among several patterns during the  
 170 competition.

### 171 3.3. State transition probability reveals the switching pattern for expertise

172 Figure 4 shows that the offensive and defensive maneuvers could be classified into six  
 173 coordination patterns and that these patterns switched over short time scales. To clarify the  
 174 characteristics of the expert and intermediate switching patterns, the histograms of the return maps  
 175 for each group were calculated. As a result, we identified two discrete states in each histogram:  
 176 the “farthest apart” high-velocity state (F) and the “nearest (closest) together” low-velocity state  
 177 (N). Figure 5 shows the second-order state transition diagrams for experts and intermediates. We

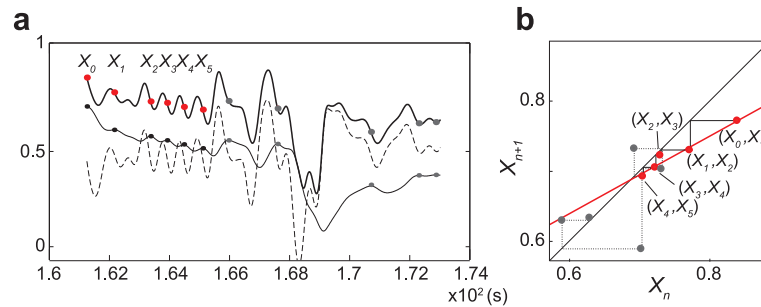


**Figure 3.** Procedure for depicting the return map from the time series of state variables. (a) Gray, broken, and black lines show the time series for normalized  $X_{IPD}(t)$ , normalized  $V_{IPD}(t)$ , and  $X(t)$ , respectively, for a 12-s trial with more than five peaks. The red and gray circles indicate the corresponding values of  $X(t)$  for the peaks of  $X_{IPD}(t)$ . (b) Return map of the time series for the observed data,  $X_n$  vs.  $X_{n+1}$  using the amplitude of  $X(t)$  at the peaks of  $X_{IPD}(t)$  corresponding to the series of points (red and gray circles) in the panel shown in a. Modified from [37].

178 identified four trajectories, such as  $\{X_n = F, X_{n+1} = F\}$ ,  $\{X_n = N, X_{n+1} = N\}$ ,  $\{X_n = F, X_{n+1} = N\}$ ,  
 179 and  $\{X_n = N, X_{n+1} = F\}$ , as second-order transitions.

180 The conditional probabilities for second-order state transitions of the experts were  $\{Pr(F|F) =$   
 181  $0.96, Pr(N|F) = 0.04\}$ , and  $\{Pr(N|N) = 0.19, Pr(F|N) = 0.81\}$ . The probabilities for intermediates  
 182 were  $\{Pr(F|F) = 0.82, Pr(N|F) = 0.18\}$ , and  $\{Pr(N|N) = 0.69, Pr(F|N) = 0.31\}$ . The transition  
 183 probabilities between experts and intermediates were clearly different; experts were more often in the  
 184 “farthest apart” high-velocity F-state. In contrast, the intermediate players remained more in the  
 185 “nearest (closest) together” low-velocity N-state.

186 The return map analysis revealed that the coordination patterns repeated over short time scales  
 187 during interpersonal competitive behavior. In addition, the state transition probability analysis  
 188 revealed differences in the switching patterns between experts and intermediates. Nevertheless, all  
 189 patterns were shown in both levels of players. However, we considered two players as one system  
 190 in these analyses. In other words, the two players were an autonomous, self-excited system. As a  
 191 result, this approach clarified how the coordination pattern between the two players behaved rather  
 192 than how the individuals behaved. How the individual adapts to abrupt changes in the external  
 193 environment must be examined for the individual perspective.

#### 194 4. Continuous to discrete dynamics: Switching dynamics

##### 195 4.1. Switching dynamics

196 The behavior of the individual is generated based on the behavior of other individuals during  
 197 interpersonal coordination. Thus, a model with temporal external input must be considered to  
 198 describe the behavior of the individual who adapts to changes in other individuals and/or the  
 199 environment. In other words, the behavior of the individual must be considered a non-autonomous,  
 200 excited system with external input. We applied switching dynamics to describe the behavior of the  
 201 individual corresponding to temporal input [38,39].

202 A Poincaré map was used to simplify the analysis of the differential equation by reducing it to  
 203 an iterated map [33]. A periodic trajectory with initial conditions within a section of the phase space  
 204 leaves that section, and the point at which this trajectory first returns to that section is determined.  
 205 This section is called Poincaré section. Three-dimensional flow maps the two-dimensional Poincaré  
 206 section, and the Poincaré map can be analyzed to understand the characteristics of the original system.  
 207 A Poincaré map is a discrete dynamical system with a phase space that is one dimension smaller than  
 208 the original continuous dynamical system. Switching dynamics applies the Poincaré map to reduce  
 209 the dimensionality of continuous dynamics.

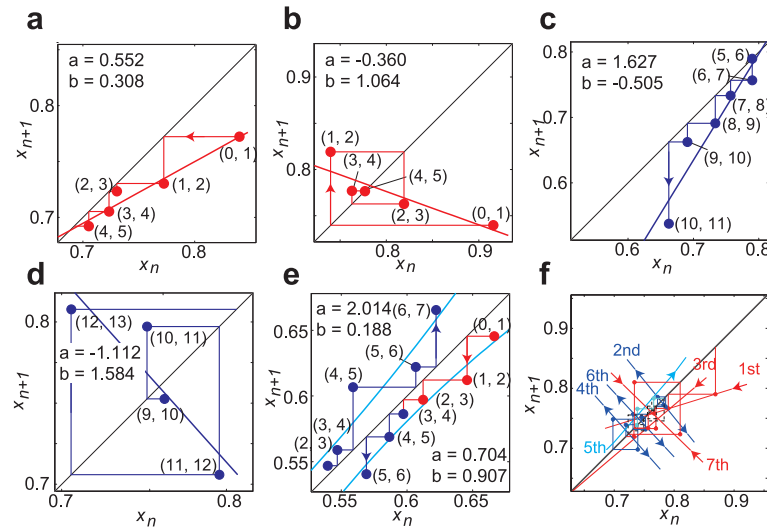


**Figure 4.** Examples of a well-fitted series of points by each function using the return map analysis. (a-d) Linear functions,  $X_{n+1} = a X_n + b$ , with four different slopes for  $0 < a < 1$ ,  $-1 < a < 0$ ,  $1 < a$ , and  $a < -1$ , respectively. (e) Exponential function,  $X_{n+1} = b \exp(a X_n)$ , and logarithmic function,  $X_{n+1} = a \log(X_n) + b$ . (f) Examples of switching functions in one scene. Red lines show attractors, blue lines show repellers, and cyan lines show intermittencies. Modified from [37].

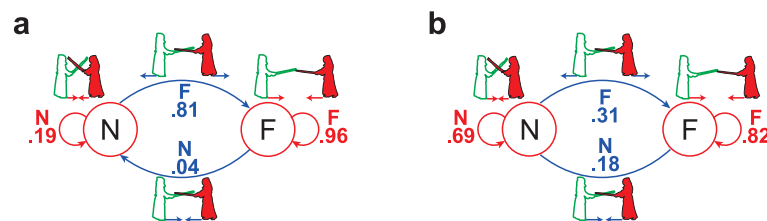


**Figure 5.** Second-order state transition diagrams with the conditional probabilities consisting of the “farthest apart” high velocity states (F) and the “nearest together” low velocity state (N) for expert (a) and intermediate (b) competitors, respectively. Modified from [37].

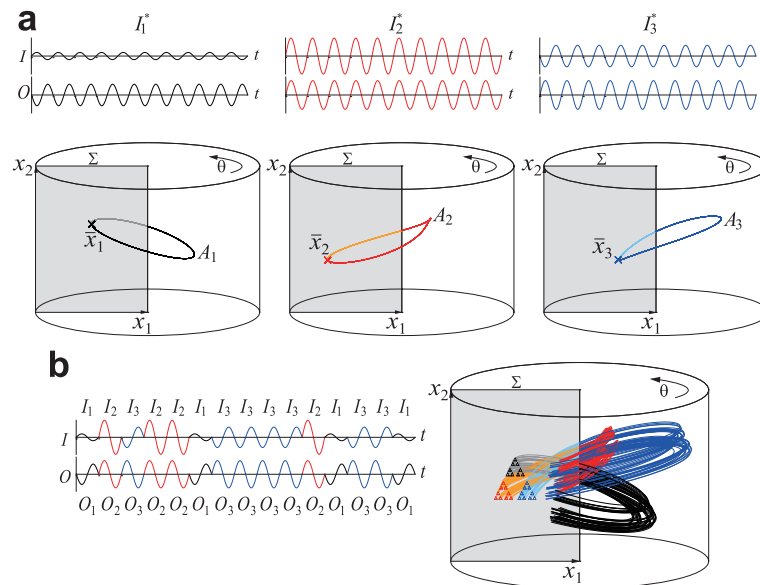


**Figure 6.** (a) Examples of time series for three periodic inputs.  $I$  and  $O$  denote input and output time series, respectively. The trajectories for three periodic inputs in three-dimensional cylindrical phase space,  $(x_1, x_2, \theta) \in \mathcal{M} : \mathbb{R}^2 \times S^1$ , corresponding to the colored trajectories denoted by  $A_1$ ,  $A_2$  and  $A_3$  cross the Poincaré section  $\Sigma : \mathbb{R}^2$  at  $\bar{x}_1$ ,  $\bar{x}_2$  and  $\bar{x}_3$ , respectively. (b) An example of a time series for switching inputs. (d) The trajectories of randomly switching inputs and the cross points on the Poincaré section show the Sierpinski gasket as a result of the fractal transitions. Modified from, with permission, [39].

210 Figure 6a shows the trajectories for three periodic inputs, such as  $I_1^*$ ,  $I_2^*$ , and  $I_3^*$ . These inputs  
 211 are changed periodically to different amplitudes with the same period. Three limit cycle attractors,  
 212 i.e., excited attractors,  $A_1$ ,  $A_2$ , and  $A_3$ , are observed in the cylindrical phase space  $\mathcal{M}$ . When the  
 213 three inputs are switched stochastically into the system, the trajectories switched corresponding to the  
 214 input. The Poincaré section shows the Sierpinski gasket (Figure 6b). All trajectories are considered to  
 215 represent the transition between the excited attractors, called the fractal transition between the excited  
 216 attractors, to characterize the dynamics of the dissipative dynamical system excited by the temporal  
 217 inputs.

#### 218 4.2. The Poincaré map reveals the underlying simple rule for the complex striking action

219 We applied these switching dynamics to the striking action during tennis to understand complex  
 220 human movements [40]. Two kinds of trajectories occurred when the ball was launched to the  
 221 forehand or backhand side repeatedly as a periodic input condition, which were termed excited  
 222 attractors, according to the input type (Figure 7a). When the ball was launched to the forehand and  
 223 backhand sides randomly as a switching input condition, the trajectories in the cylindrical phase  
 224 space were more complex (Figure 7b).

225 To understand the behavior of the system, we examined the Poincaré map on the Poincaré  
 226 section,  $\Sigma$ , as discrete dynamics. Figure 8a shows the set of points on the Poincaré section under  
 227 a periodic input condition corresponding to the Figure 7a. Figure 8b shows the set of points on the  
 228 Poincaré section during a switching input condition corresponding to the Figure 7b, and Figure 8c  
 229 shows the ellipse of the constant distance by using the mean and  $\pm 1$  *S.D.* for the switching input  
 230 condition. The characteristic configurations of the four clusters of sets on the Poincaré sections  
 231 corresponded to the Cantor set with rotation. Figure 8d shows the return map of the Cantor set  
 232 with rotation leaving from the initial state,  $x_0$ , when the first input was the backhand side, the next  
 233 state,  $x_{1B}$ , and returned to B in Figure 8d. When the second input was the backhand side, the next

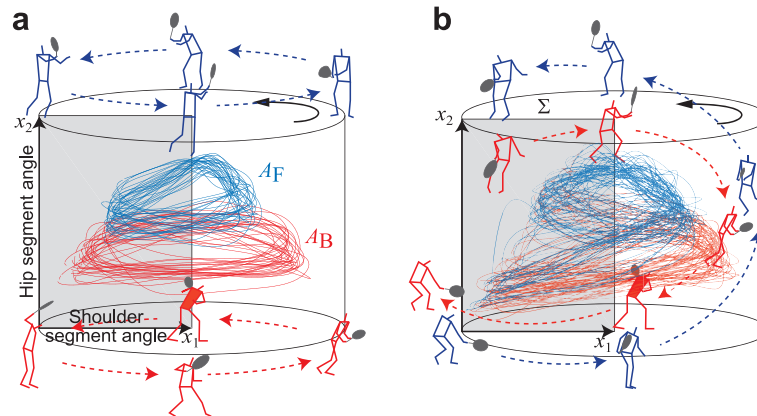


**Figure 7.** The trajectories in three-dimensional cylindrical phase space. (a) Periodic input condition, (b) switching input condition. Stick pictures show forehand and backhand striking movements at each point in time series. Modified from, with permission, [40].

234 state,  $x_{2B}$ , returned to BB. In contrast, when the second input was the forehand side, the next state,  
 235  $x_{2F}$ , returned to BF. The behavior of the system was understood as the time evolution of the Cantor set  
 236 with rotation (Figure 8e). In other words, the time evolution of the striking action corresponding to  
 237 the two input types was characterized as a fractal transition of the Cantor set. These findings suggest  
 238 that a simple rule underlying a complex human behavior can be understood as discrete dynamics by  
 239 reducing the continuous dynamics using a Poincaré map analysis.

## 240 5. Switching hybrid dynamics

241 As mentioned above, the coordination modes of interpersonal competitive behavior can be  
 242 examined as a synchronization phenomena of two-coupled nonlinear oscillators or as continuous  
 243 dynamics. However, interpersonal competitive behavior shows abrupt changes in coordination  
 244 modes, which differs from rhythmic interlimb coordination (e.g., [1]) or interpersonal coordination  
 245 (e.g., [6]). The distribution of the relative phase region analysis reveals the characteristics of the  
 246 global coordination mode without considering time evolution. Thus, it does not describe the local  
 247 coordination patterns on a shorter time scale. To solve this problem, the interpersonal competitive  
 248 patterns on a short time scale were classified using a return map analysis, referring to the Lorenz  
 249 map and reducing the dimensionality from continuous dynamics to discrete dynamics. Furthermore,  
 250 the switching among patterns was determined by state transition probabilities and revealed the  
 251 characteristics of experts. This finding suggests that continuous interpersonal competitive behavior,  
 252 which seem to be a complex phenomenon, includes both perception of each other and their own  
 253 decision making, and the two players execute their actions depending on their decisions. In other  
 254 words, interpersonal competitive behavior can be regarded as a continuous switching pattern on  
 255 a shorter time scale. In martial arts, such as boxing or fencing, the two players can move freely  
 256 around each other; thus, the behavior of a system comprised of two players is a weakly coupled  
 257 oscillator system [8,26,33]. Thus, collective variables can be defined to describe the state of the system  
 258 during continuous dynamics (Figure 3). Underlying simple rules can be identified in interpersonal  
 259 competitive behavior using a return map as discrete dynamics (Figure 5). This perspective shows the  
 260 interactive behavior as a whole system.

261 Another perspective to understand interpersonal competitive behavior is to view part of the  
 262 system in the whole by focusing on individual behavior. Then, other movements are regarded as  
 263 external input patterns or environmental changes, and the individual would generate their output  
 264 patterns according to their input patterns. This means that the system is considered non-autonomous.  
 265 The switching dynamics model suggests that the output pattern would be generated by switching  
 266 among several input patterns [38,39]. Behavior during court-net sports is constrained by the

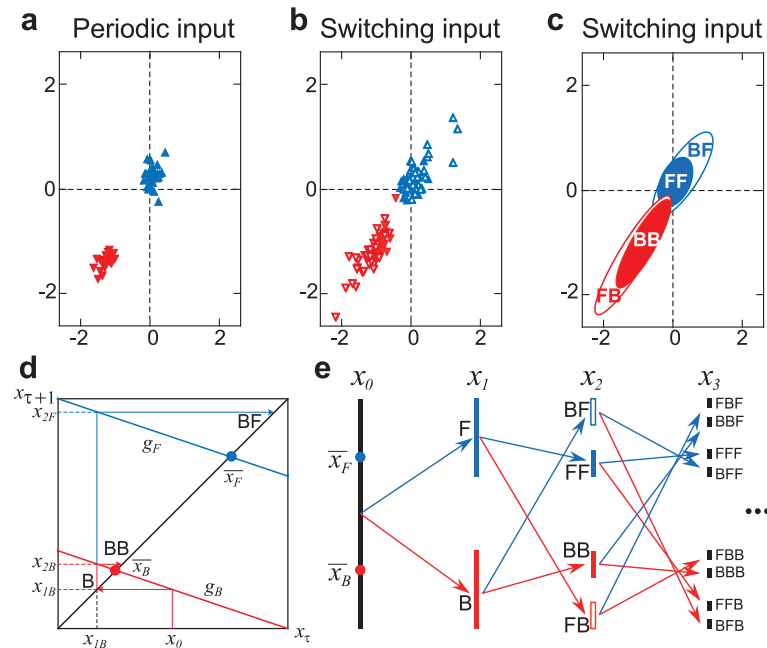


**Figure 8.** Examples of Poincaré sections  $\Sigma$  for the periodic and switching input conditions. (a) Periodic input, (b) switching input, and (c) the ellipse of constant distance using each mean and  $\pm 1$  S.D. for switching input. (d) This shows how the Cantor set  $C$  with rotation is constructed using two iterative functions. The iterative functions  $g_F$  and  $g_B$  transform the state,  $x_\tau$ , to the next state,  $x_{\tau+1}$ . The transformations of the iterative functions  $g_F$  and  $g_B$  are rotated around the fixed points  $x_F$  and  $x_B$ , respectively. (e) The hierarchical structure of the fractal corresponds to the sequence of forehand (F) and backhand (B) inputs. Modified, with permission, from [40].

267 movement of the ball hit by the opponent. In this case, each individual is a non-autonomous system,  
 268 and the underlying simple rules could be identified as discrete dynamics (Figure 8), and complex  
 269 individual behavior as continuous dynamics (Figure 7).

270 The proposed integrated model is the switching hybrid dynamical system [41]. Here, we assume  
 271 a system with a higher module and a lower module, which interact with each other by switching  
 272 inputs from the higher to the lower module, and by using a feedback signal from the lower to the  
 273 higher module. In addition, external input feeds into the higher module, as shown in Figure 9.

$$\text{Discrete dynamical system: } I_l(t); l = \sigma(I_{ext}(t), x(t)) \quad (4)$$

$$\text{Continuous dynamical system: } \dot{x} = f_l(x(t), I_l(t)) \quad (5)$$

274 Here, the discrete dynamical system  $I_l(t)$  is the higher module corresponding to the brain and  
 275 prefrontal cortex [42,43], and the continuous dynamical system  $\dot{x}$  is the lower module corresponding  
 276 to the human motor system. This system focuses on the individual **A** during competition between  
 277 **A** and **B**. The higher module transforms into human movement based on the continuous output  
 278 pattern from the opponent **B**,  $I_{ext}(t)$  and the final state of the lower module  $x(t)$ . The higher module  
 279 considers one of three patterns  $I_l(t)$  and transforms into movement. Thus, when the movement  
 280 pattern of the opponent **B** switches among the three patterns, the movement patterns of **A** will show  
 281 three fractal trajectory subsets. However, the pattern determined by **A** is not always consistent with  
 282 the continuous output pattern from the opponent **B**,  $I_{ext}(t)$ . Because higher brain functions, such  
 283 as selective attention [44–47], the visual search strategy [48–50], and decision making [51–53] are  
 284 redundant due to neuronal redundancy of cell assemblies [54], the same external input  $I_{ext}(t)$  does  
 285 not always generate the same decision  $I_l(t)$ . This problem might be related to expertise.

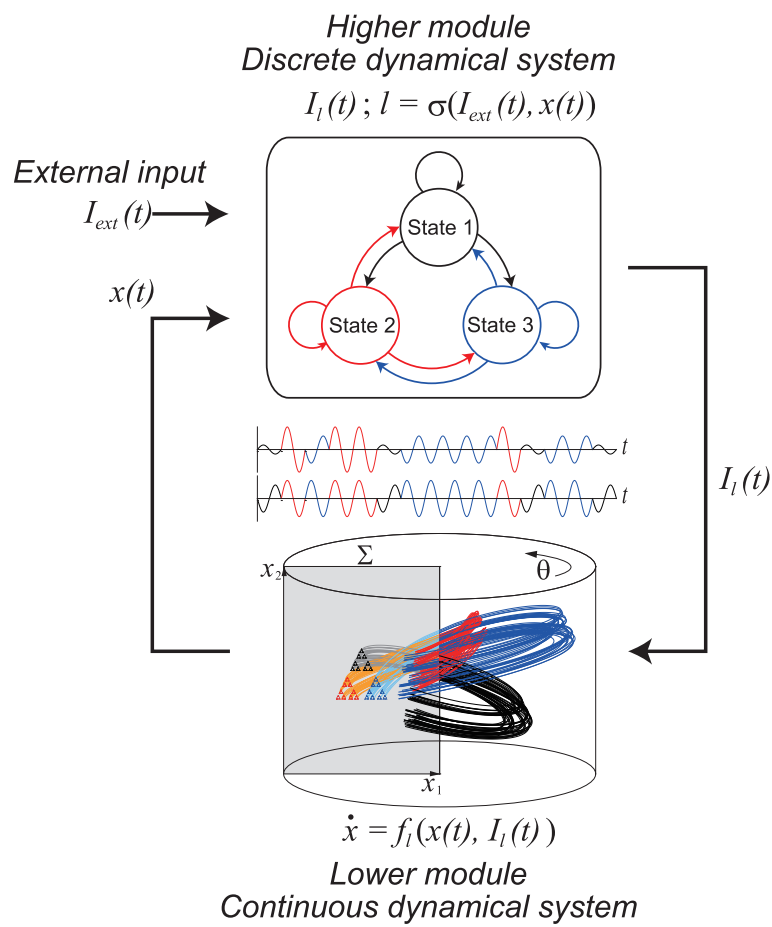


**Figure 9.** Schematic representation of switching hybrid dynamics, which is composed of a discrete dynamical system as a higher module and a continuous dynamical system as a lower module with a feedback loop. This system is non-autonomous.

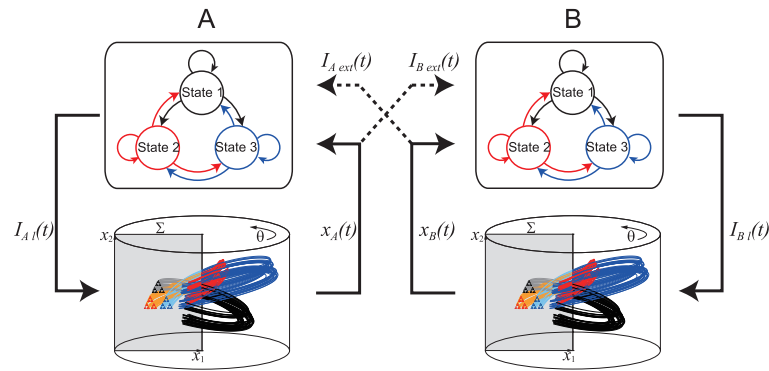


**Figure 10.** Schematic representation for two-coupled switching hybrid dynamics. This system is autonomous.

286 When the external inputs feed into the system, system outputs of the continuous dynamical  
 287 system are generated regularly depending on continuous switching of external inputs  $I_{ext}(t)$  and  
 288 the final states of the system  $x(t)$ , as shown in section 4.2. This suggests that behavior of the system  
 289 shows hysteresis and can be used to predict the next state. However, it has been confirmed that the  
 290 regularities differ according to the length of time of the external input [55–57]. In this case, we focused  
 291 on individual behavior during an interpersonal competitive situation; that is, we regarded the system  
 292 as non-autonomous.

293 When these two systems are connected to each other, it is regarded as an autonomous system as  
 294 a whole (Figure 10). That is, the final state of the other system,  $x_A(t)$  in **A** and  $x_B(t)$  in **B**  
 295 transforms into external input for the system  $I_{Bext}(t)$  in **B** and  $I_{Aext}(t)$  in **A**, respectively. As a result, the two  
 296 systems are connected through external inputs. Then, the behavior of the whole system is described  
 297 as:  $\dot{X} = F(X), X = (x_A, x_B)$ . In the case of kendo matches, the behavior of the whole system has  
 298 been described as the instantaneous relative phase difference of the step toward-away movements  
 299 of the two players. However, six offensive and defensive maneuver patterns have been found, and  
 300 these patterns switch continuously during a kendo match, suggesting that the regularity underlying  
 301 switching among competitive patterns could be clarified if these patterns are regarded as output  
 302 patterns and/or external input patterns using slightly longer time windows. However, the regularity  
 303 remained unclear after determining the state transition probabilities for the competitive patterns.  
 304 Applying switching hybrid dynamics to interpersonal competitive behavior would help to clarify  
 305 how the behavior will be generated during the time course as a whole system.

## 306 6. Conclusion

307 We investigated how to examine the underlying dynamics of complex interpersonal competitive  
 308 behavior during sport activities using the continuous dynamical system, which was described  
 309 by differential equations, and the discrete dynamical system, which was described by difference  
 310 equations and/or iterated maps. Weakly coupled sports, such as boxing, fencing, and kendo, in which  
 311 the players move relatively freely regardless of the opponent's movement, were examined using  
 312 a two-coupled nonlinear oscillator mode. Then, the order and control parameters were identified  
 313 and the coordination modes between the two players were determined. Furthermore, because these  
 314 continuous dynamics could be reduced to discrete dynamics using iterated maps, the coordination  
 315 patterns in interpersonal competitive behavior could be depicted on shorter time scales. On the other  
 316 hand, in strongly coupled sports, such as court-net sports in which movements of the players are  
 317 constrained by movement of the ball hit by the opponent, the regularities in the evolution of the  
 318 system were clarified using the switching dynamical system with external temporal input, which  
 319 reduced the dimensionality based on the Poincaré map.

320 The proposed switching hybrid dynamical system was applied not only to court-net sports, such  
 321 as tennis or table tennis, but also to weakly coupled sports, such as boxing or fencing, to understand  
 322 the regularities underlying the interpersonal competitive behavior. However, further theoretical and  
 323 behavioral examinations will be needed. Additionally, the team sports applications, which require  
 324 both intra-team coordination and inter-team competition, is a next step.

325 **Acknowledgments:** We thank Kazutoshi Kudo for helpful comments and discussions that improved the  
 326 manuscript. This work was partially supported by Grants-in-Aid for Scientific Research (A) 24240085 and  
 327 25242059 from MEXT, Japan and a Grant-in-Aid for Challenging Exploratory Research 16K12994 from the JSPS,  
 328 Japan.

329 **Author Contributions:** YY, AK, MO, KY, and KG were equally contributed to all parts of this manuscript; the  
 330 ideas, theoretical frameworks and writing.

331 **Conflicts of Interest:** The authors declare no conflict of interest. The founding sponsors had no role in the design  
 332 of the study; in the collection, analyses, or interpretation of data; in the writing of the manuscript, and in the  
 333 decision to publish the results.

### 334 References

- 335 1. Kelso, J.A.S. Phase transitions and critical behavior in human bimanual coordination. *American Journal of*  
 336 *Physiology* **1984**, *246*, R1000–R1004.
- 337 2. Bennett, M.; Schatz, M.F.; Rockwood, H.; Wiesenfeld, K. Huygens' clock. *Proceedings of the Royal Society*  
 338 *A: Mathematical, Physical and Engineering Sciences* **2002**, *458*, 563–579.
- 339 3. Strogatz, S. *SYNC: The emerging science of spontaneous order*; Hyperion Books: New York, 2003.
- 340 4. Haken, H.; Kelso, J.A.S.; Bunz, H. A theoretical model of phase transitions in human hand movements.  
 341 *Biological Cybernetics* **1985**, *51*, 347–356.
- 342 5. Haken, H. *Synergetics: An introduction, non-equilibrium phase transitions and self-organization in physics,*  
 343 *chemistry and biology*, 2nd ed.; Springer: Berlin, 1978.
- 344 6. Schmidt, R.C.; Carello, C.; Turvey, M.T. Phase transitions and critical fluctuations in the visual  
 345 coordination of rhythmic movements between people. *Journal of Experimental Psychology: Human*  
 346 *Perception and Performance* **1990**, *16*, 227–247.
- 347 7. Schmidt, R.C.; Turvey, M.T. Phase-entrainment dynamics of visually coupled rhythmic movements.  
 348 *Biological Cybernetics* **1994**, *70*, 369–376.
- 349 8. Kuramoto, Y. *Chemical oscillations, waves, and turbulence*; Springer-Verlag: Berlin, 1984.
- 350 9. Nédá, Z.; Ravasz, E.; Brechet, Y.; Vicsek, T.; Barabási, A.L. Self-organizing processes: the sound of many  
 351 hands clapping. *Nature* **2000**, *403*, 850–851.
- 352 10. Frank, T.D.; Richardson, M.J. On a test statistics for the Kuramoto order parameter of synchronization:  
 353 an illustration for group synchronization during rocking chairs. *Physica D* **2010**, *239*, 2084–2092.
- 354 11. Richardson, M.J.; Garcia, R.L.; Frank, T.D.; Gergor, M.; Marsh, K.L. Measuring group synchrony: a  
 355 cluster-phase method for analyzing multivariate movement time-series. *Frontiers in Physiology* **2012**,  
 356 *3*, 405.
- 357 12. Aihara, I.; Takeda, R.; Mizumoto, T.; Otsuka, T.; Takahashi, T.; Okuno, H.G.; Aihara, K. Complex and  
 358 transitive synchronization in a frustrated system of calling frogs. *Physical Review E* **2011**, *83*, 031913.
- 359 13. Golubitsky, M.; Stewart, I. *The symmetry perspective: from equilibrium to chaos in phase space and physical*  
 360 *space*; Birkhäuser Verlag: Basel, Switzerland, 2002.
- 361 14. Yokoyama, K.; Yamamoto, Y. Three people can synchronize as coupled oscillators during sports activities.  
 362 *PLoS Computational Biology* **2011**, *7*, e1002181.
- 363 15. Gray, R. 'Markov at the bat': A model of cognitive processing in baseball batters. *Psychological Science*  
 364 **2002**, *13*, 542–547.
- 365 16. McGarry, T.; Franks, I.M. A stochastic approach to predicting competition squash match-play. *Journal of*  
 366 *Sports Sciences* **1994**, *12*, 537–584.
- 367 17. McGarry, T.; Franks, I. Development, application, and limitation of a stochastic Markov model in  
 368 explaining championship squash performance. *Research Quarterly for Exercise and Sport* **1996**, *67*, 406–415.
- 369 18. Kelso, J.A.S. *Dynamic patterns: The self-organization of brain and behavior*; The MIT Press: Cambridge, MA,  
 370 1995.

- 371 19. Coey, C.; Varlet, M.; Schmidt, R.C.; Richardson, M.J. Effects of movement stability and congruency on the  
372 emergence of spontaneous interpersonal coordination. *Experimental Brain Research* **2011**, *211*, 483–493.
- 373 20. Fine, J.M.; Amazeen, E.L. Interpersonal Fitts' law: when two perform as one. *Experimental Brain Research*  
374 **2011**, *211*, 459–469.
- 375 21. Richardson, M.J.; Marsh, K.L.; Schmidt, R.C. Effects of visual and verbal interaction on unintentional  
376 interpersonal coordination. *Journal of Experimental Psychology: Human Perception and Performance* **2005**,  
377 *31*, 62–79.
- 378 22. Schmidt, R.C.; O'Brien, B. Evaluating the dynamics of unintended interpersonal coordination. *Ecological*  
379 *Psychology* **1997**, *9*, 189–206.
- 380 23. Yamanishi, J.; Kawato, M.; Suzuki, R. Two coupled oscillators as a model for the coordinated finger  
381 tapping by both hands. *Biological Cybernetics* **1980**, *37*, 219–225.
- 382 24. Scholz, J.P.; Kelso, J.A.S. A quantitative approach to understanding the formation and change of  
383 coordinated movement patterns. *Journal of Motor Behavior* **1989**, *21*, 122–144.
- 384 25. Pikovsky, A.; Rosenblum, M.; Kurths, J. Phase synchronization in regular and chaotic system: a tutorial.  
385 *International Journal of Bifurcation and Chaos* **2000**, *10*, 2291–2306.
- 386 26. Pikovsky, A.; Rosenblum, M.; Kurths, J. *Synchronization: a universal concept in nonlinear sciences*;  
387 Cambridge University Press: New York, 2001.
- 388 27. Carvalho, J.; Araújo, D.; Travassos, B.; Esteves, P.; Pessanha, L.; Pereira, F.; Davids, K. Dynamics of players  
389 relative positioning during baseline rallies in tennis. *Journal of Sports Sciences* **2013**, *31*, 1596–1605.
- 390 28. Lames, M. Modelling the interaction in game sports - relative phase and moving correlations. *Journal of*  
391 *Sports Science and Medicine* **2006**, *5*, 556–560.
- 392 29. Palut, Y.; Zanone, P.G. A dynamical analysis of tennis: concepts and data. *Journal of Sports Sciences* **2005**,  
393 *23*, 1021–1032.
- 394 30. McGarry, T. Identifying patterns in squash contests using dynamical analysis and human perception.  
395 *International Journal of Performance Analysis in Sport* **2006**, *6*, 134–147.
- 396 31. Chow, J.Y.; Seifert, L.; Héroult, R.; Chia, S.J.Y.; Lee, M.C.Y. A dynamical system perspective to  
397 understanding badminton singles game play. *Human Movement Science* **2014**, *33*, 70–87.
- 398 32. Yamamoto, Y.; Okumura, M.; Yokoyama, K.; Kijima, A. 13. Interpersonal Coordination in Competitive  
399 Sports Contexts: Martial Arts. In *Interpersonal Coordination and Performance in Social Systems*; Passos, P.;  
400 Davids, K.; Chow, J.Y., Eds.; Routledge: Oxford, UK, 2016; pp. 179–194.
- 401 33. Strogatz, S.H. *Nonlinear dynamics and chaos*; Westview Press: Cambridge, MA, 1994.
- 402 34. Okumura, M.; Kijima, A.; Kadota, K.; Yokoyama, K.; Suzuki, H.; Yamamoto, Y. A critical interpersonal  
403 distance switches between two coordination modes in kendo matches. *PLoS ONE* **2012**, *7*, e51877.
- 404 35. Kijima, A.; Kadota, K.; Yokoyama, K.; Okumura, M.; Suzuki, H.; Schmidt, R.C.; Yamamoto, Y. Switching  
405 dynamics in an interpersonal competition brings about 'Deadlock' synchronization of players. *PLoS ONE*  
406 **2012**, *7*, e47911.
- 407 36. Lorenz, E.N. Deterministic nonperiodic flow. *Journal of Atmospheric Sciences* **1963**, *20*, 130–141.
- 408 37. Yamamoto, Y.; Yokoyama, K.; Okumura, M.; Kijima, A.; Kadota, K.; Gohara, K. Joint action syntax in  
409 Japanese martial arts. *PLoS ONE* **2013**, *8*, e72436.
- 410 38. Gohara, K.; Okuyama, A. Dynamical systems excited by temporal inputs: Fractal transition between  
411 excited attractors. *Fractals* **1999**, *7*, 205–220.
- 412 39. Gohara, K.; Okuyama, A. Fractal transition: Hierarchical structure and noise effect. *Fractals* **1999**,  
413 *7*, 313–326.
- 414 40. Yamamoto, Y.; Gohara, K. Continuous hitting movements modeled from the perspective of dynamical  
415 systems with temporal input. *Human Movement Science* **2000**, *19*, 341–371.
- 416 41. Nishikawa, J.; Gohara, K. Automata on fractal sets observed in hybrid dynamical systems. *International*  
417 *Journal of Bifurcation and Chaos* **2008**, *18*, 3665–3678.
- 418 42. Miller, E.K. The prefrontal cortex and cognitive control. *Nature Reviews Neuroscience* **2000**, *1*, 59–65.
- 419 43. Sakagami, M.; Tsutsui, K. The hierarchical organization of decision making in the primate prefrontal  
420 cortex. *Neuroscience Research* **1999**, *34*, 79–89.
- 421 44. Ditzinger, T.; Haken, H. Oscillations in the perception of ambiguous patterns. *Biological Cybernetics* **1989**,  
422 *61*, 279–287.

- 423 45. Drew, T.; Vö, M.L.H.; Wolfe, J.M. The invisible Gorilla strikes again: sustained inattentional blindness in  
424 expert observers. *Psychological Science* **2013**, *24*, 1848–1853.
- 425 46. Gregoriou, G.G.; Gotts, S.J.; Zhou, H.; Desimone, R. High-frequency, long-range coupling between  
426 prefrontal and visual cortex during attention. *Science* **2009**, *324*, 1207–1210.
- 427 47. Neisser, U.; Becklen, R. Selective looking: attending to visually specified events. *Cognitive Psychology*  
428 **1975**, *7*, 480–494.
- 429 48. Alder, D.; Ford, P.R.; Causer, J.; Williams, A.M. The coupling between gaze behavior and opponent  
430 kinematics during anticipation of badminton shots. *Human Movement Science* **2014**, *37*, 167–179.
- 431 49. Vaeyens, R.; Lenoir, M.; Philippaerts, R.M.; Williams, A.M. Mechanisms underpinning successful decision  
432 making in skilled youth soccer players: an analysis of visual search behaviors. *Journal of Motor Behavior*  
433 **2007**, *39*, 395–408.
- 434 50. Williams, A.M.; Ward, P.; Knowles, J.M.; Smeeton, N.J. Anticipation skill in a real-world task:  
435 measurement, training, and transfer in tennis. *Journal of Experimental Psychology: Applied* **2002**, *8*, 259–270.
- 436 51. Araújo, D.; Davids, K.; Serpa, S. An ecological approach to expertise effects in decision-making in a  
437 simulated sailing regatta. *Psychology of Sport and Exercise* **2005**, *6*, 671–692.
- 438 52. Araújo, D.; Davids, K.; Hristovski, R. The ecological dynamics of decision making in sport. *Psychology of*  
439 *Sport and Exercise* **2006**, *7*, 653–676.
- 440 53. Thura, D.; Cos, I.; Trung, J.; Cisek, P. Context-dependent urgency influences speed-accuracy trade-offs in  
441 decision making and movement execution. *Journal of Neuroscience* **2014**, *34*, 16442–16454.
- 442 54. Buzsáki, G. Neural syntax: cell assemblies, synapsesemblies, and readers. *Neuron* **2010**, *68*, 362–385.
- 443 55. Hirakawa, T.; Suzuki, H.; Okumura, M.; Gohara, K.; Yamamoto, Y. Switching dynamics between two  
444 movement patterns varies according to time interval. *International Journal of Bifurcation and Chaos* **2016**,  
445 *26*, 1630026.
- 446 56. Hirakawa, T.; Suzuki, H.; Gohara, K.; Yamamoto, Y. Inverse proportional relationship between  
447 switching-time length and fractal-like structure for continuous tracking movement. *International Journal*  
448 *of Bifurcation and Chaos* **2017**, *27*, 1730040.
- 449 57. Suzuki, H.; Yamamoto, Y. Robustness to temporal constraint explains expertise in ball-over-net sports.  
450 *Human Movement Science* **2015**, *41*, 193–206.